Effect of interdiffusion and magnetic field on two-electron states in Gaussian-shaped double quantum rings

V.L. Aziz-Aghchegala, V.N. Mughnetsyan, A.A. Kirakosyan

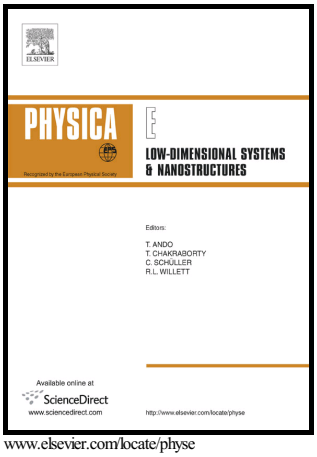

www.elsevier.com/locate/physe

PII: S1386-9477(16)31303-0
DOI: http://dx.doi.org/10.1016/j.physe.2017.01.005
Reference: PHYSE12693

To appear in: *Physica E: Low-dimensional Systems and Nanostructures*

Received date: 11 November 2016
Revised date: 12 December 2016
Accepted date: 3 January 2017

Cite this article as: V.L. Aziz-Aghchegala, V.N. Mughnetsyan and A.A. Kirakosyan, Effect of interdiffusion and magnetic field on two-electron states i Gaussian-shaped double quantum rings, *Physica E: Low-dimensional System and Nanostructures,* http://dx.doi.org/10.1016/j.physe.2017.01.005

Effect of interdiffusion and magnetic field on two-electron states in Gaussian-shaped double quantum rings

V.L. Aziz-Aghchegala[a],* V.N. Mughnetsyan[b], and A.A. Kirakosyan[b]
[a] *Department of Physics, Urmia Branch, Islamic Azad University, Urmia, Iran,*
[b] *Department of Solid State Physics, Yerevan State University, Alex Manoogian 1, 0025 Yerevan, Armenia*

The effects of interdiffusion and electrons' Coulomb interaction on the energy spectrum in Gaussian-shaped single and double quantum rings in the presence of magnetic field has been considered in the framework of exact diagonalization method. The one-electron energies as functions of magnetic field for different values of diffusion parameter have been obtained. The two-electron energies and electron probability density distributions are obtained as well. It is shown that the energy oscillations which are more pronounced for a single quantum ring, smooth out due to the interdiffusion. The Coulomb interaction transforms the crossings of the two-electron levels to anticrossings and can lead to the appearance of an additional level between the anticrossing levels.

Keywords: Gaussian-shaped quantum ring, magnetic field, interdiffusion, Coulomb interaction

I. INTRODUCTION

Recently, the zero dimensional quantum dot (QD) heterostructures, or so called artificial atoms, containing few interacting electrons have attracted the most attention among the semiconductor nanostructures because of applications in novel devices and the rich physics they exhibit [1]. Just as the QDs, quantum rings (QR) confine electrons in three directions, but the topology of QRs differs from one of QDs leading to new phenomena, predicted by theory and observed in experiments. The observation of the Aharonov-Bohm oscillations [2] and the persistent current [3–6] in small conducting rings in the presence of external magnetic field, and recent experimental realization of QRs with only a few electrons [7, 8], have made QRs an attractive topic of experimental research and a new playground for the many-particle theory [9, 10]. The pioneering experiment of Lorke, et. al. [8] demonstrated that most of their rings contained just two electrons. Hence, QRs containing two interacting electrons have received considerable attention in recent years [11–14]. The effects of electron-electron interaction on the persistent current in a mesoscopic QR subjected to a magnetic field was discussed by Chakraborty and Pietilainen [12, 15]. Theoretical studies on the optical-absorption spectra of a QD have been presented by Hallonen et al. [16], taking into account repulsive scattering centers. The effect of the electron-impurity Coulomb interaction (CI) on the Aharonov-Bohm oscillations has also been studied in [17]. In reference [18] the use of external time-dependent magnetic field for the control of the quantum states in a two-electron quantum ring has been investigated. It was shown that the singlet-triplet transitions take place when magnetic field was changed and suitable magnetic field values and time scales was evaluated for efficient quantum ring control. In [19] it is shown that two-electron states in a QR can be described analytically under a certain conditions. Besides the external fields the internal structural changes, such as interdiffusion between the compound materials of heterostructure (which can be induced by post growth rapid thermal annealing) can also be an effective tool for controlling the structure parameters [20–23]. Theoretical calculations [24, 25] indicate to the increase of QDs absorption threshold due to interdiffusion, which is in accordance with the experimentally observed blueshift of photoluminescence spectrum [23]. Our previous works are devoted to the theoretical investigation of the effect of interdiffusion on electronic band structure and absorption spectrum of QRs and QR superlattices which can be successfully used in the intermadiate band solar cells [26–29]. In [27] and [28] we have used the model of Gaussian-shaped double quantum ring (GSDQR) for more realistic description of such objects obtained in experiment [29]. In this paper we present the theoretical investigation of the effect of interdiffusion and Coulomb interaction on one- and two-electron states in $GaAs/Ga_{1-x}Al_xAs$ Gaussian-shaped QRs subjected to an external magnetic field.

II. THEORY

The single electron Hamiltonian in a GSDQR in the presence of transversal magnetic field can be written in the following form:

$$\hat{H}(\vec{r}) = \hat{H}_0(\vec{r}) + V_G(r,z;L) - \frac{\imath}{2}\hbar\omega_B\frac{\partial}{\partial\varphi} + \frac{1}{8}m^*\omega_B^2 r^2 + \frac{1}{2}g\mu_B B, \quad (1)$$

were H_0 is the Hamiltonian of electron in cylindrical quantum dot (CQD) with infinitely high potential barriers and with enough large radius R_0 and height h_0, m^* is electron effective mass,

$$V_G(r,z;L) = V_0\left(1 - \frac{1}{2}erf\left(\frac{z}{L}\right) - \exp\left(-\frac{r^2}{L^2}\right)\times \frac{1}{L^2}\int_0^\infty erf\left(\frac{z(t)-z}{L}\right) I_0\left(\frac{2rt}{L^2}\right)\exp\left(-\frac{t^2}{L^2}\right) tdt\right) \quad (2)$$

* Corresponding author: v.aziz@iaurmia.ac.ir

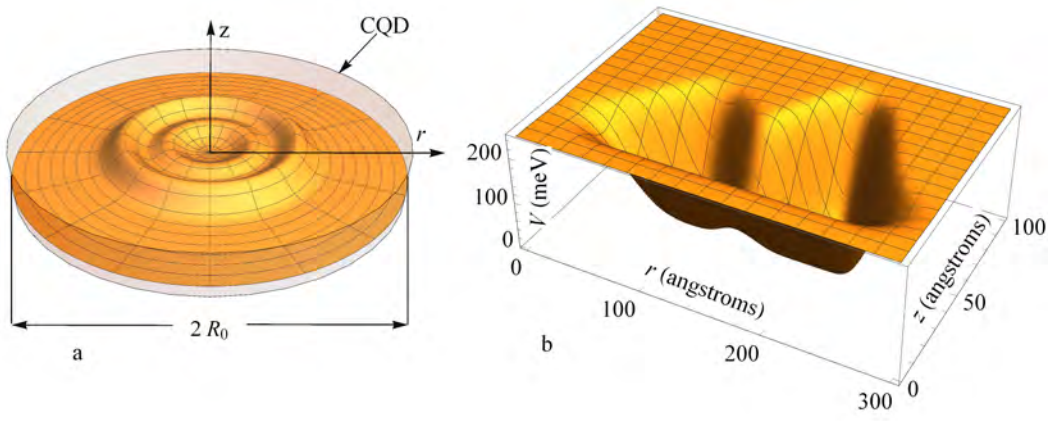

FIG. 1. (Colour on-line) The shape (a) and the potential profile (b) of the GSDQR

is the potential of GSDQR which is obtained as a solution of Fick's equation. In formulas (1)–(2) $L = 2\sqrt{D\tau}$ is the diffusion parameter, D is diffusion coefficient, τ is time, $V_0 = 1247Qx$meV is the potential barriers' height before the interdiffuison (x is the Al initial concentration and $Q = 0.6$ is the conduction band offset for GaAs material) [27, 28], $erf(\xi)$ is the error function, ω_B is the cyclotron frequency, μ_B is the Bohr magneton, B is the magnetic field induction which is directed along the QR's z axis, g is the Landé g-factor, I_0 is the modified Bessel function of zero order. The surface which covers the GSDQR can be expressed by the following dependence of z coordinate on the radial coordinate r:

$$z(r) = h_1 \exp[-\alpha^2(r - r_1)^2] + h_2 \exp[-\beta^2(r - r_2)^2], \quad (3)$$

were α, β, h_1 and h_2 are Gaussian parameters, r_1 and r_2 are the values of r at which the inner and the outer Gaussians have maximum respectively. To obtain the energy spectrum for the Hamiltonian (1) we imply the exact diagonalization method using the eigenfunctions of H_0 as an ansatz:

$$\psi_1 = \sum_q c_q \phi_q(z, r, \varphi), \quad (4)$$

were

$$\phi_q(z, r, \varphi) = \left(\frac{2}{h_0}\right)^{1/2} \sin\left(\frac{\pi n_z z}{h_0}\right) \times \frac{1}{\pi^{1/2} R_0 J_{|l|+1}(k_{n,l})} J_l\left(k_{n,l}\frac{r}{R_0}\right) \exp(il\varphi) \quad (5)$$

are the eigenfunctions of H_0, J_l is the first kind Bessel function of the l-th order and q denotes the complect of the quantum numbers n_z, n and l. The two-electron Hamiltonian in a material with dielectric constant ε in the presence of magnetic field and the CI is

$$H(\vec{r}_1, \vec{r}_2) = H(\vec{r}_1) + H(\vec{r}_2) + \frac{e^2}{\varepsilon|\vec{r}_2 - \vec{r}_1|}, \quad (6)$$

and the corresponding wave function is sought as the following superposition:

$$\Psi(\vec{r}_1, \vec{r}_2) = \sum_{q_1 < q_2} C_{q_1,q_2} \psi_{2,q_1,q_2}(\vec{r}_1, \vec{r}_2), \quad (7)$$

were the antisymmetric wave function

$$\psi_{2,q_1,q_2}(\vec{r}_1, \vec{r}_2) = \psi_{q1}(\vec{r}_1)\psi_{q2}(\vec{r}_2) - \psi_{q1}(\vec{r}_2)\psi_{q2}(\vec{r}_1) \quad (8)$$

is used as an ansatz [30]. The probability density (PD) distribution can be obtained by integration of the two-electron wave function modulus square by one of the coordinates:

$$P(\vec{r}) = \int |\Psi(\vec{r}, \vec{r}_i)|^2 d\vec{r}_i, \quad (9)$$

and the mean square distance (MSD) between electrons is expressed as follows [31]:

$$MSD = \int \Psi^*(\vec{r}_1, \vec{r}_2)(\vec{r}_2 - \vec{r}_1)^2 \Psi(\vec{r}_1, \vec{r}_2) d\vec{r}_1 d\vec{r}_2, \quad (10)$$

III. RESULTS AND DISCUSSION

A. Interdiffusion

The numerical calculations are made for the values of parameters $m^* = 0.067m_0$ (m_0 is the free electron mass), $\varepsilon = 12.9$ and $x = 0.33$. We use the values of the electron effective mass and the dielectric constant for GaAs material because electrons are mainly localized in QR.

In Fig.1 the shape of GSDQR (a) and the profile of its diffused potential (b) are illustrated for the values of parameters: $h_1 = 30$Å, $h_2 = 50$Å, $R_0 = 1.5R$, $r_1 = R/3$, $r_2 = 2R/3$, $\alpha = \beta = 0.025$Å^{-1}, $L = 10$Å and $R = 300$Å. The CQD, the eigenfunctions in which are used

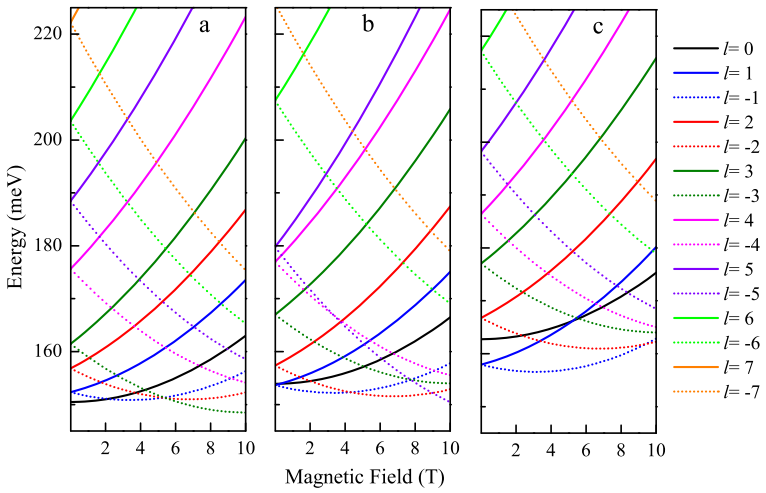

FIG. 2. (Colour on-line) Dependencies of the electron energies corresponding to the value of the radial quantum number $n = 1$ on magnetic field induction in GSDQR for the values of the diffusion parameter $L = 0$ (a), $L = 5$Å (b) and $L = 10$Å (c).

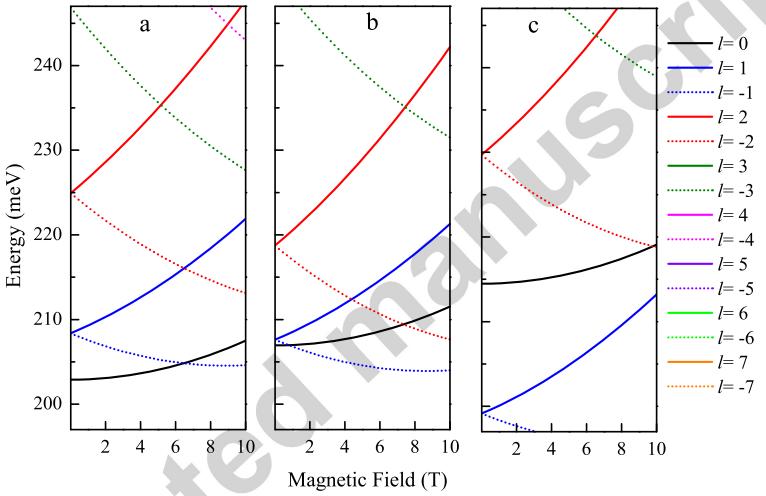

FIG. 3. (Colour on-line) Dependencies of the electron energies corresponding to the value of the radial quantum number $n = 2$ on magnetic field induction in GSDQR for the values of the diffusion parameter $L = 0$ (a), $L = 5$Å (b) and $L = 10$Å (c).

as an ansatz for the diagonalization of the matrix of the Hamiltonian (6), is also presented in Fig.1a. As it is seen the radius and the height of CQD are large enough to provide the convergence of the real wave function in the barrier region. We can also see from Fig.1b that the value of the diffussion parameter $L = 10$Å corresponds to an intermediate situation when the profile of the potential is smoothed but still two QRs exist.

Figs.2 and 3 demonstrate the dependencies of the electron energies corresponding to the values of the radial quantum number $n = 1$ and $n = 2$, respectively, for different values of the azimuthal quantum number l on magnetic field induction in GSDQR. Three different values of the diffusion parameter $L = 0$ (a), $L = 5$Å (b) and $L = 10$Å (c) have been considered. As is seen from the figures the change in the energy has an oscillating character due to the crossings of the levels corresponding to different values of l. However clear Aharonov-Bohm oscillations are not observed mainly because of the considerable tunneling of electron to the region near the QR axis. The dept of the confining potential decreases due to interdiffusion leading to the up-shift of the ground state energy levels (Figs.2b, c and Figs.3b, c), but the higher levels are shifted down (Figs.3b, c) or the up-shift is weaker in comparison with the ground state (Figs.2b, c) because of the enlargement of the potential in the re-

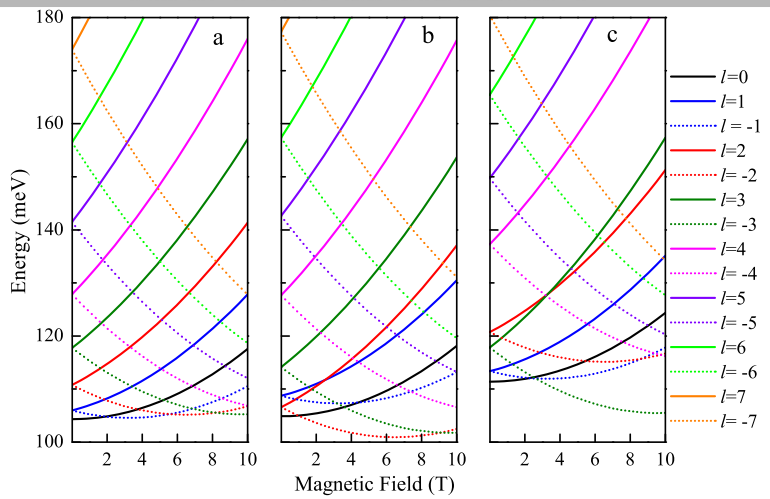

FIG. 4. (Colour on-line) Dependencies of the electron energies corresponding to the value of the radial quantum number $n = 1$ on magnetic field induction in single GS QR for the values of the diffusion parameter $L = 0$ (a), $L = 5$Å (b) and $L = 10$Å (c).

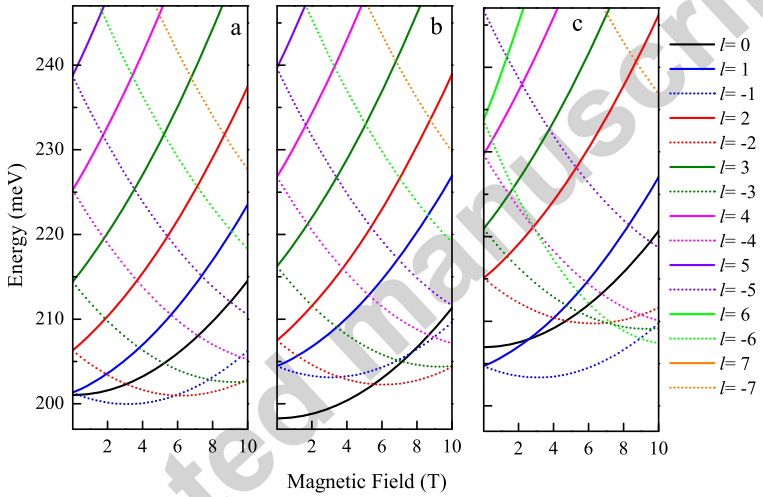

FIG. 5. (Colour on-line) Dependencies of the electron energies corresponding to the value of the radial quantum number $n = 2$ on magnetic field induction in single GS QR for the values of the diffusion parameter $L = 0$ (a), $L = 5$Å (b) and $L = 10$Å (c).

gion of higher energies and the merge of the inner and the outer rings. So the interdiffusion changes the sequence of the energy levels. One can also note a non-monotonic change of the energies of some levels (for example the levels corresponding to the values of quantum numbers $n = 1, l = \pm 5$ in Fig.2 and $n = 2, l = \pm 2$ in Fig.3) with the increase of the diffusion parameter. Namely, these energies decrease at the intermediate value of diffusion parameter $L = 5$Å due to the merge of the inner and the outer rings and after increase due to the decrease of the depth of the confining potential. One can also conclude that the oscillating behavior of the magnetic field dependencies of low energy levels gradually disappears with the increase of diffusion parameter because of the enhanced tunneling of electron to the central region of the ring.

Figs.4 and 5 show the same dependencies as in Figs.2 and 3 for a Gaussian-shaped single QR (GSSQR) with the values of parameters $h_1 = 0$, $h_2 = 70$Å, and $\beta = 0.2$Å^{-1}. The ground state energy oscillations due to crossings in the case of $L = 0$ (Fig.4a and Fig.5a) are more pronounced comparing with the corresponding ones in Fig.2a and Fig.3a due to the ring-like topology of the structure (the tunneling to the central region of QR is very weak). However the interdiffusion distorts the picture of oscillations like in the above considered case (Figs.2 and 3).

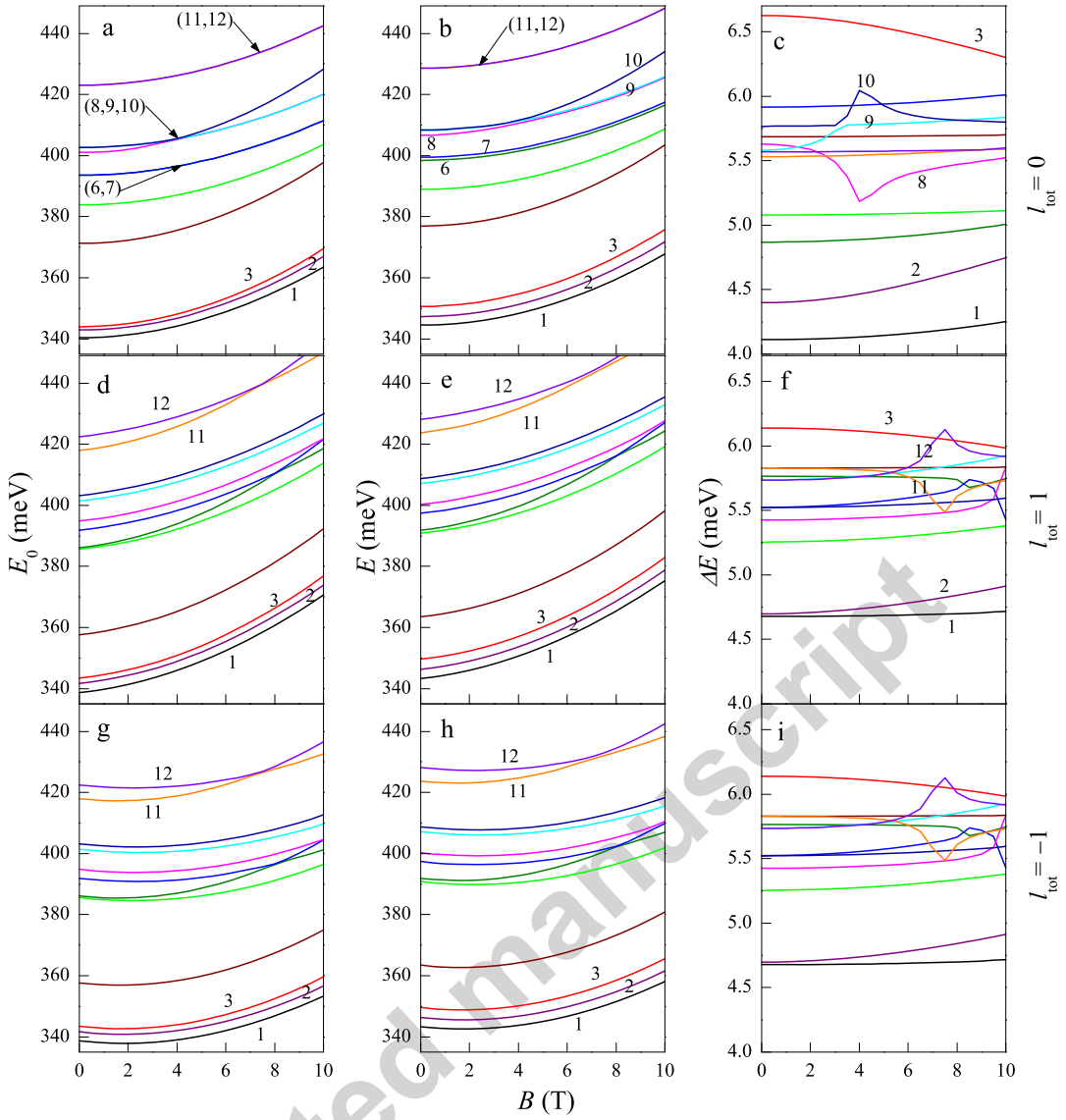

FIG. 6. (Colour on-line) Energy of triplet states without (a, d, g) and with (b, e, h) taking into account the CI and the differences of these energies (c, f, i) as functions of the magnetic field induction.

B. Coulomb Interaction

The numerical calculations for the two-electron energies in GSDQR have been done for the following values of parameters: $h_1 = 30$Å, $h_2 = 50$Å, $R_0 = 1.5R$, $r_1 = R/3$, $r_2 = 2R/3$, $\alpha = \beta = 0.025$Å^{-1} and $R = 300$Å. Here we consider the case of the GSDQR with non diffused potential profile ($L = 0$) to enforce the main peculiarities of the CI. In Fig.6 the dependencies of the energies of two-electron triplet states on magnetic field induction with (E) and without (E_0) taking into account the CI between electrons as well as the Coulomb corrections (CC) of the energy $\Delta E = E - E_0$ are presented. Figs.6a, b and c correspond to the value of the total azimuthal quantum number $l_{tot} = 0$, while the Figs.6d, e and f and the Figs.6g, h and i correspond to the values of $l_{tot} = 1$ and $l_{tot} = -1$ respectively. Like in the case of one-electron states the increase of the energies for $l_{tot} = 1$ takes place more rapidly comparing with the case of $l_{tot} = 0$, whereas there is a region of decrease of the energy for $l_{tot} = -1$ due to the negative interaction energy of the electron magnetic moment with the external field. It is clear that in all cases there is a positive shift of the energies due to CI which is in the range of about $4 - 6.5$meV (Figs.6c, f, i). One can easily observe the identity of the curves in Fig.6f and i because of the same spatial distribution of the electronic probability in the cases of $l_{tot} = 1$ and $l_{tot} = -1$. It is also clear that the range of the values of

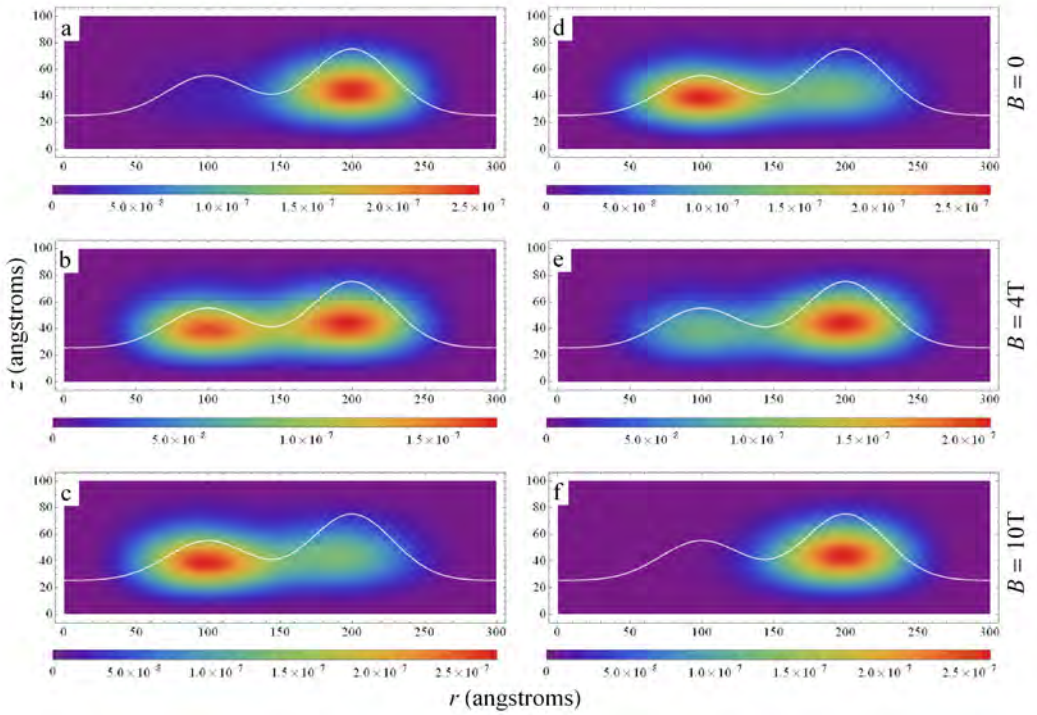

FIG. 7. (Colour on-line) PD distributions of two-electrons as functions of the radial and the axial coordinates for $l_{tot} = 0$ and for the values of magnetic field induction $B = 0$ (a, d), $B = 4$T (b, e) and $B = 10$T (c, f). The white line is the profile of the GSDQR.

CC is larger when $l_{tot} = 0$ due to the more flexibility of the radial distribution of the probability with respect to the magnetic field.

Comparing Figs.6a, d and g with Figs.6b, e and h, respectively, one can see that CI leads to the "repulsion" of the first three states due to the additional quantization. However, for high-laying states this regularity is not observed which is obvious from the fact that the sequence of the curves in Figs.6c, f and i do not coincides with one in Figs.6b, e and h. This can be explained by moving away of electrons via the CI-enhanced tunneling through the barrier region between the rings. The increase of the CC for the first two states with the increase of magnetic field is due to the increase of the electrons localization, while the decrease of the CC for the third state (red line in Figs.6c, f, i) is due to the quantum ejection of one of electrons from the inner ring to the outer one. It is seen from the Figs.6a, d and g that there are crossings of some levels (8-th and 10-th levels for $l_{tot} = 0$, 6-th and 7-th or 11-th and 12-th levels for $l_{tot} = \pm 1$) if the CI is not taken into account. However, these crossings transform to anticrossings when we add the CI term in the Hamiltonian (Figs.6b, e and h) because the CI removes the degeneracy of the states at the crossing points. It should be mentioned that in the absence of CI for $l_{tot} = 0$ there is a threefold degeneracy at $B \simeq 4T$ for the 8-th, 9-th and 10-th states. Moreover, the 9-th level coincides with the 10-th level when $B < 4T$ and it coincides with 8-th one when $B > 4T$ (Fig.6a). However, if one takes into account the CI, three levels with different energies are observed (the purple, light blue and royal lines in Fig.6b). In other words the 9-th level is an additional level which appears due to CI. There are also degeneracies observed in whole range of the values of magnetic field for the 6-th and the 7-th levels as well as for the 11-th and the 12-th levels in the case of $l_{tot} = 0$ which is also removed by CI. It is clear from Figs.6c, f and i that the CC has a maximum or a minimum at crossing points ($B = 4$T for $l_{tot} = 0$ and $B = 7.5$T for $l_{tot} = \pm 1$).

To understand the nature of these extrema let us consider the Figs.7, 8 and 9. Fig.7 represents the PDs for the 8-th (Figs.7a, b and c) and the 10-th (Fig.7d, e and f) levels as functions of the radial (r) and the axial (z) coordinates when $l_{tot} = 0$ for three different values of magnetic field induction: $B = 0$ (a and d), $B = 4$T (b and e) and $B = 10T$ (c and f), while on Fig.8 the PDs are presented for the 11-th (Fig.8a, b and c) and the 12-th (Fig.8d, e and f) levels when $l_{tot} = \pm 1$ for $B = 0$ (a and d), $B = 7.5$T (b and e) and $B = 10$T (c and f). It is clear from Fig.7 that at $B = 4T$ there are two separated maxima of PD indicating on a spatial separation of electrons in contrast with the cases of $B = 0$ and $B = 10$T. That is why the corresponding dependence of CC (Fig.6c) has a minimum. However for the 10-th level there is only one maximum which shifts from the inner ring to the outer one with the increase of B. In other words the minimal

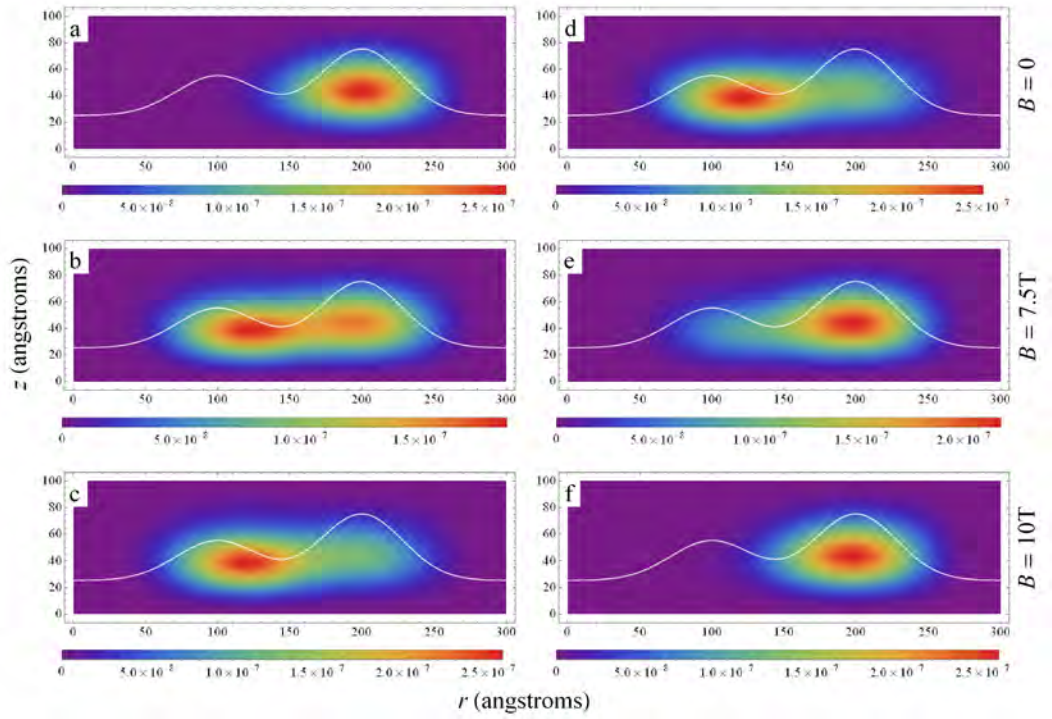

FIG. 8. (Colour on-line) PD distributions of two-electrons as functions of the radial and the axial coordinates for $l_{tot} = \pm 1$ and for the values of magnetic field induction $B = 0$ (a, d), $B = 7.5$T (b, e) and $B = 10$T (c, f). The white line is the profile of the GSDQR.

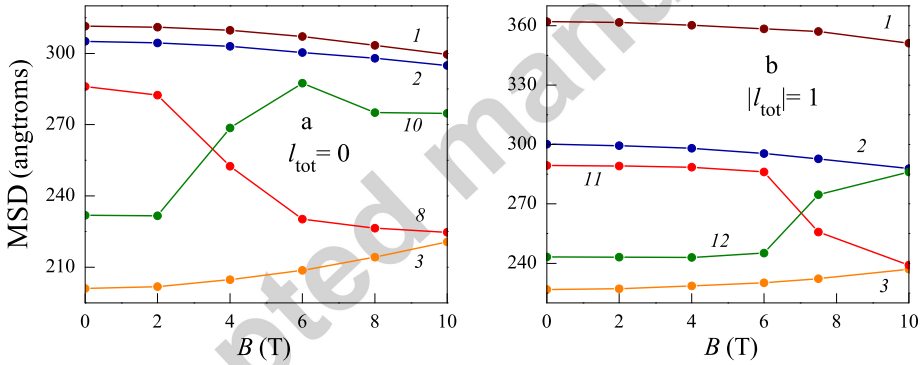

FIG. 9. (Colour on-line) MSD of the electrons for the values of the total azimuthal momentum $l_{tot} = 0$ (a) and $l_{tot} = \pm 1$ (b).

correlation between electrons for one of the crossing levels corresponds to the maximal correlation for the other one. One can observe similar behavior for the 11-th and 12-th levels when $l = \pm 1$ (Fig.8). The comparison of Fig.7 and Fig.8 shows that the PD of the higher levels is smoothed out and the penetration of electrons into the barrier region between the rings is stronger in comparison with the lower levels. The change in electrons' correlation in GSDQR has also been observed in [32] by varying the distance between the inner and the outer rings which have a similar impact on the tunneling as the change of magnetic field. Similar PDs have also been obtained for a QR with volkano-like shape in [33].

In Fig.9 the MSDs of the electrons are presented for the levels 1, 2, 3, 8 and 10 at $l_{tot} = 0$ (Fig.9a) and for the levels 1, 2, 3, 11 and 12 at $l_{tot} = \pm 1$ (Fig.9b) as functions of magnetic field induction. We see that in both cases (a and b) the MSD decreases with the increase of B for 1-st and the 2-nd levels, while the MSD for the 3-rd level increases, which is in the accordance with the corresponding curves (the black, violet and the red lines) in Figs.6c, f and i. Note that the curves corresponding to the MSD of the two crossing levels intersect near the points $B = 4$T when $l_{tot} = 0$ and $B = 7.5$T when $l_{tot} = \pm 1$. From comparison of the Fig.9a with Fig.6c, or the Fig.9b with Fig.6f one can conclude that the behav-

ior of the CC can not be explained only via the effect of the CI energy (the extremes of the CC are not extremes for MSD) but the quantum coupling between the 8-th and the 10-th levels (or between the 11-th and the 12-th levels) should also be taken into account. For example the coupling of the 8-th and the 10-th levels leads to the higher quantization for the 10-th level (with corresponding CC maximum) and to the lower quantization for the 8-the level (with corresponding CC minimum).

IV. CONCLUSION

Summarizing, the effect of interdiffusion and electrons' Coulomb interaction on the energy spectrum in GSSQR and GSDQR in the presence of axial magnetic field has been considered in the framework of exact diagonalization method. The one-electron energies as functions of magnetic field for different values of diffusion parameter have been obtained. The two-electron triplet state energies, Coulomb corrections, probability density distributions and mean square distances between electrons in GSDQR are obtained as well. It is shown that the energy oscillations, being more pronounced for a single QR, are however vanished due to the interdiffusion. The crossings of the two-electron levels transform to anticrossings due to the Coulomb interaction. Moreover, when the total angular momentum is zero the Coulomb interaction can cause to the appearance of an additional level between the anticrossing levels. The probability density of the 8-th (11-th) level in the case of $l_{tot} = 0$ ($l_{tot} = \pm 1$) shifts from the outer ring to the inner one, while the probability density of the 10-th (12-th) level shifts in opposite direction with the increase of magnetic field, resulting to the crossing of the MSD curves of different levels.

ACKNOWLEDGMENTS

This work is the result of a research project and was supported by Urmia Branch, Islamic Azad University, Urmia, Iran. The research of A.A. Kirakosyan was supported by the RA MES State Committee of Science, in the frames of the research project 15T-1C363. The research of V.N. Mughnetsyan was supported by RA MES State Committee of Science, in the frames of the research project 15T-1C331 and by Armenian National Science and Education Fund (ANSEF) grant nano-4199. The authors are also grateful to Dr. Aram Manaselyan for valuable discussions.

[1] T. Chakraborty, *Quantum Dots* (North-Holland, Amsterdam, 1999); P.A. Maksym and T. Chakraborty, Phys. Rev. Lett. **65**, 108 (1990).
[2] Y. Aharonov, D. Bohm, Phys. Rev. **115**, 485 (1959).
[3] M. Büttiker, Y. Imry, R. Landauer, Phys. Lett. A **96**, 365 (1983).
[4] L.P. Levy, G. Dolan, J. Dunsmuir, and H. Bouchiat, Phys. Rev. Lett. **64**, 2074 (1990).
[5] V. Chandrasekhar, R.A. Webb, M.J. Brady, M.B. Ketchen, W.J. Gallagher, and A. Kleinsasser, Phys. Rev. Lett. **67**, 3578 (1991).
[6] D. Mailly, C. Chapelier, and A. Benoit, Phys. Rev. Lett. **70**, 2020 (1993).
[7] R.J. Warburton, et. al, Nature **405**, 926 (2000).
[8] A. Lorke, et. al, Phys. Rev. Lett. **84**, 2223 (2000).
[9] T. Chakraborty, Adv. in Solid State Phys. **43**, 79,(2003).
[10] S. Viefers, P. Koskinen, P. Singha Deo, M. Manninen, Physica E **21**, 1 (2004).
[11] P. Pietilainen and T. Chakraborty, Solid State Commun. **87**, 809 (1993).
[12] T. Chakraborty and P. Pietilainen, Phys. Rev. B **50**, 8460 (1994).
[13] L. Wendler, V.M. Fomin, A.V. Chaplik, and A. O. Govorov, Phys. Rev. B **54**, 4794 (1996).
[14] Y. Liu, et. al, Phys. Rev. B **82**, 045312 (2010).
[15] T. Chakraborty and P. Pietilainen, Phys. Rev. B **52**, 1932 (1995).
[16] V. Hallonen, P. Pietilainem, and T. Chakraborty, Europhys. Lett. **33**, 377 (1996).
[17] M.G. Barseghyan, A.Kh. Manaselyan, D. Laroze, A.A. Kirakosyan, Physica E, **81**, 31 (2016).
[18] J. Sarkka, A. Harju, Physica E **42**, 844 (2010).
[19] N.G. Aghekyan, E.M. Kazaryan, L.S. Petrosyan, H.A. Sarkisyan, J. Phys., Conference Series **248**, 012048 (2010).
[20] R. Leon, S. Fafard, P. G. Piva, S. Ruvimov, Z. Lilietal-Weber, Phys. Rev. B **58**, R4262 (1998)
[21] T.K. Ng, H.S. Djie, S.F. Yoon, T. Mei, J. Appl. Phys. **97**, 013506 (2005).
[22] A. Agarwal, M. Srujan, S. Chakrabarti, S. Krishna, J. Lumin. **143**, 96 (2013).
[23] Y. Ji, W. Lu, G. Chen, X.S. Chen, Q. Wang, J. Appl. Phys. **93**, 1208 (2003).
[24] J.A. Barker, E.P. O'Railly, Physica E **4**, 231 (1999).
[25] O. Gunawan, H.S. Djie, B.S. Ooi, Phys. Rev. B **71**, 205319 (2005).
[26] V.L. Aziz-Aghchegala, V.N. Mughnetsyan, A.A. Kirakosyan, Physica E **64**, 51 (2014).
[27] V.L. Aziz-Aghchegala, V.N. Mughnetsyan, A.A. Kirakosyan, Physica E **65**, 30 (2015).
[28] V.L. Aziz-Aghchegala, V.N. Mughnetsyan, A.A. Kirakosyan, Physica E **70**, 210 (2015).
[29] J. Wu, Z.M. Wang, V.G. Dorogan, S. Li, J. Lee, Y.I. Mazur, E.S. Kim, G.J. Salamo, Nanoscale Res. Lett. **8**, 5 (2013).
[30] A. Manaselyan, A. Ghazaryan, T. Chakraborty, Solid State Communications, **181**, 34 (2014).
[31] F.M. Peeters, V.A. Schweigert, Phys. Rev. B **53**, 1468 (1995).
[32] J.I. Climente, J. Planelles, M. Barranco, F. Malet, M. Pi, Phys. Rev. B **73**, 235327 (2006).
[33] V.V. Arsoski, M.Ž. Tadić, F.M. Peeters, Phys. Rev. B **87**, 085314 (2013).